

6. A. J. Wagers, I. L. Weissman, *Cell* **116**, 639 (2004).
 7. M. LaBarge, H. M. Blau, *Cell* **111**, 589 (2002).
 8. J. G. Fox *et al.*, *Cancer Res.* **62**, 696 (2002).
 9. Materials and methods are available as supporting material on Science Online.
 10. P. H. Schmidt *et al.*, *Lab. Invest.* **79**, 639 (1999).
 11. J. R. Goldenring *et al.*, *Gastroenterology* **118**, 1080 (2002).
 12. G. P. Boivin *et al.*, *Gastroenterology* **124**, 762 (2003).
 13. A. D. Clouston, *Pathology* **33**, 271 (2001).
 14. J. G. Fox *et al.*, *Cancer Res.* **63**, 942 (2003).
 15. R. Okamoto *et al.*, *Nature Med.* **8**, 1011 (2002).
 16. Q. Li, S. M. Karam, J. I. Gordon, *J. Biol. Chem.* **271**, 3671 (1996).
 17. D. Normille, *Science* **298**, 1869 (2002).
 18. J. Couzin, *Science* **299**, 1002 (2003).
 19. N. Serakinci *et al.*, *Oncogene* **23**, 5095 (2004).
 20. We thank K. Cormier and the Division of Comparative Medicine histology lab for technical support and expertise in IHC, and D. Altieri and E. Kurt-Jones for their helpful comments and suggestions. Supported by NIH grants K22 CA90518 (J.H.), RO1 CA87958 (T.C.W. and J.G.F.), RO1 DK58889 (T.C.W.), and a VA

Merit Review and Vanderbilt GI SPORE 1P50 CA95103 (J.R.G.).

Supporting Online Material
www.sciencemag.org/cgi/content/full/306/5701/1568/DC1
 Materials and Methods
 Figs. S1 to S6
 Table S1

23 April 2004; accepted 7 October 2004

Nucleosome Arrays Reveal the Two-Start Organization of the Chromatin Fiber

Benedetta Dorigo,^{1*} Thomas Schalch,^{1*} Alexandra Kulangara,¹ Sylwia Duda,¹ Rasmus R. Schroeder,² Timothy J. Richmond^{1†}

Chromatin folding determines the accessibility of DNA constituting eukaryotic genomes and consequently is profoundly important in the mechanisms of nuclear processes such as gene regulation. Nucleosome arrays compact to form a 30-nanometer chromatin fiber of hitherto disputed structure. Two competing classes of models have been proposed in which nucleosomes are either arranged linearly in a one-start higher order helix or zigzag back and forth in a two-start helix. We analyzed compacted nucleosome arrays stabilized by introduction of disulfide cross-links and show that the chromatin fiber comprises two stacks of nucleosomes in accord with the two-start model.

DNA in eukaryotic cell nuclei assembles with histone proteins into chromatin (1). The nucleosome constitutes the first level of organization (2, 3). The “30-nm” chromatin fiber consists of nucleosome arrays in their most compact form and is typically posited as the second structural level of DNA organization (4). The hierarchy continues with increasing DNA-packing density until the metaphase chromosome is attained (5). The structure of the 30-nm fiber, or nucleosome higher order structure, has been contentious for two decades. Most models have in common that an open zigzag string of nucleosomes self-assembles into a helical structure ~30 nm in diameter. The models can be grouped into two classes: (i) the one-start helix, with bent linker DNA connecting each pair of nucleosome cores, which follow each other immediately along the same helical path (6) (Fig. 1A), and (ii) the two-start helix, based on straight linker DNA connecting between two adjacent stacks of helically arranged nucleosome cores (7). The most prominent representative of the one-start class is the

solenoid, where the nucleosomes coil around a central cavity with ~six to eight nucleosomes per turn (8–10). The two-start class is divided between two main models named the helical ribbon model (7, 11) (Fig. 1B) and the crossed-linker model (12) (Fig. 1C).

With the aim of elucidating the higher-order structure of compact nucleosome arrays, we developed an *in vitro* system for producing highly regular arrays incorporating all recombinant components (13). With these arrays, we

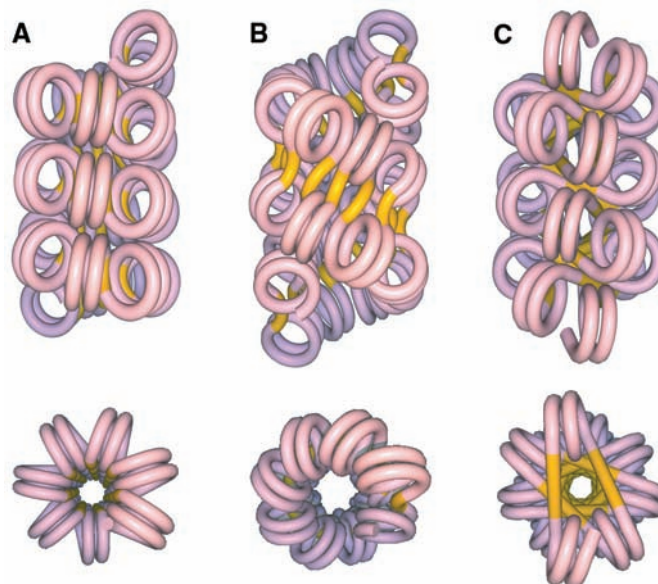
have shown that the base of the histone H4 tail is crucial for compaction. The crystal structure of the nucleosome core particle reveals that this region (amino acids 14 to 19) makes an interparticle contact with H2A/H2B of a neighboring particle (2, 3). We used this information to select a pair of cysteine-replacement mutants that stabilizes the higher order structure by disulfide formation. We constructed mutant versions of histones H2A, H2B, and H4 by replacing one selected amino acid with cysteine in each version [for H2A, Glu⁵⁶, Glu⁶¹, and Glu⁶⁴ (H2A-E56C, H2A-E61C, and H2A-E64C); for H2B, Gln⁴⁴, Val⁴⁵, and Glu¹¹⁰ (H2B-Q44C, H2B-V45C, and H2B-E110C); and for H4, Lys²⁰, Val²¹, Arg²³, and Asp²⁴ (H4-K20C, H4-V21C, H4-R23C, and H4-D24C)], and nucleosome arrays were assembled by using 12 different pairings of a mutant H4 with either a mutant H2A or H2B (table S1). The range of distances between the side-chain γ atoms of the selected pair of amino acids spans 3.8 to 9.7 Å determined from the nucleosome core structure. Cross-links were formed in solutions containing a 1:1 ratio of reduced and oxidized glutathione to promote disulfide formation without driving cross-linking irrespective of array folding. MgCl₂ at ~1 mM or ~100 mM was used to cause compaction, or alternatively the linker histone H1 was used to compact arrays in the absence of divalent cation. Initial trials cov-

¹Eidgenössische Technische Hochschule (ETH) Zürich, Institute for Molecular Biology and Biophysics, ETH-Hönggerberg, CH-8093 Zürich, Switzerland. ²Max Planck Institute for Medical Research, Department of Biomechanical Mechanisms, Jahnstrasse 29, 69120 Heidelberg, Germany.

*These authors contributed equally to this work.

†To whom correspondence should be addressed. E-mail: richmond@mol.biol.ethz.ch

Fig. 1. Models for the DNA path in the chromatin fiber. Higher order structure models: (A) one-start solenoidal (6), (B) two-start supercoiled (7), and (C) two-start twisted (12). Upper views have the fiber axis running vertically; lower views are down the fiber axis. DNA associated with the nucleosome core is red/blue, and linker DNA running between cores is yellow. These models are idealized, with nucleosome cores in each start contacting each other. The open three-dimensional zigzag seen in conditions not fully compacting may be a precursor (21).



ered a range of reaction conditions for all 12 mutant-containing arrays, but only the H4-V21C/H2A-E64C combination yielded a major cross-linked species (Fig. 2). Therefore, the H4-V21C/H2A-E64C combination was used in all subsequent experiments.

Disulfide formation in this system requires array compaction, and compaction requires inclusion of divalent cation or histone H1. Sedimentation velocity analysis shows that dodecanucleosomes containing the H4-V21C/H2A-E64C histones have a similar degree of compaction as compared to arrays containing wild-type histone sequences (13), both in the unfolded state with no divalent cation present and after crosslinking in the fully compacted state (fig. S1A). The crosslinked arrays maintain a fully compacted structure to lower divalent cation concentration as compared with the wild-type arrays (0.5 mM versus 1.0 mM MgCl₂), indicating that the disulfide bonds formed stabilize the folded, compact state (fig. S1B). Once formed, the cross-links prevent arrays from full unfolding in conditions lacking divalent cation. The diminished compaction of the mutant array compared with that of wild type in the presence of dithiothreitol (DTT) above 0.5 mM MgCl₂ indicates that H4-V21 and H2A-E64 contribute to internucleosome interaction in the folded fiber.

Cross-linked arrays can be cleaved under nonreducing conditions in each linker DNA segment by Sca I endonuclease. The maximum length of the cleaved arrays observed by native agarose-polyacrylamide gel electrophoresis (APAGE) after this treatment reveals the number of starts, or columns of nucleosomes, in the chromatin fibers. We show that, for arrays with either 12 or 10 nucleosome repeats, the maximum number of nucleosomes remaining after cross-linking and cleavage is 6 or 5, respectively (Fig. 3). We confirmed that virtually all linker DNA segments are cleaved by observing that essentially only mononucleosomes exist after reduction of cross-links with 100 mM DTT. This result demonstrates that the compacted nucleosome arrays have a two-start geometry. The nucleosomes in each start are connected by disulfide cross-links, so that after linker DNA cleavage the arrays are separated into individual nucleosome stacks that are maximally one-half the length of the starting array. For a one-start arrangement, the linker DNA and nucleosome-nucleosome cross-links would reinforce the same connectivity between nucleosomes, and therefore the longest bands expected would correspond to the uncleaved starting lengths of 12 and 10 nucleosomes, respectively. We have used arrays with different repeat lengths to demonstrate that the one-start versus two-start result is independent of DNA linker length. Furthermore, arrays with one copy of histone H1 bound per nucleosome yield the same result.

The ladders of bands observed by native APAGE for nucleosome arrays after disulfide crosslinking and Sca I cleavage indicate that not all cysteine thiol groups form crosslinks.

The maximum theoretical yield for a two-start structure given end effects and the possibility of two cross-links between adjacent nucleosomes is 83.3% for a dodecanucleosome.

Fig. 2. Internucleosome disulfide cross-linking of histones H4 and H2A with compaction of nucleosome arrays. SDS-PAGE shows that nucleosome arrays (12 repeats of 177 bp) containing histones H4-V21C and H2A-E64C yield a specific disulfide cross-link on compaction with 100 mM MgCl₂ at 37°C (lane 2) and at 22°C (lane 3). Noncompacted arrays (no MgCl₂, 0.5 mM EDTA, 37°C) under the same conditions show nearly undetectable disulfide formation (lane 6) and are comparable to starting material (lane 1). A competing internucleosome disulfide cross-link between two H4 molecules occurs for arrays compacted under conditions of 50 mM KCl and 1 mM MgCl₂ at 22°C (lane 5) but not at 37°C (lane 4). All cross-linking reactions were arrested by addition of 10 mM iodoacetamide. Cross-links within compacted arrays (lane 2) can be completely reversed after arrest by addition of 100 mM DTT (lane 7). A separate gel shows the cross-linking of a nucleosome array (10 repeats of 208 bp) with ~one histone H1 molecule bound per nucleosome (lane 8).

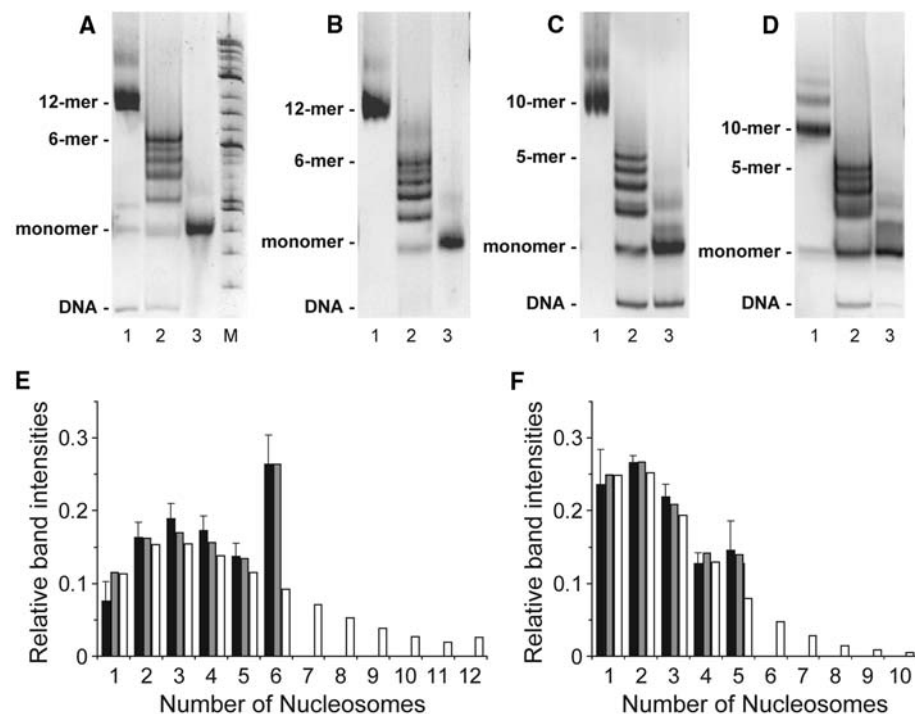


Fig. 3. Fragmentation of nucleosome arrays with Sca I after disulfide cross-linking. Nucleosome arrays containing (A) 12 repeats of 177 bp, (B) 12 repeats of 167 bp, (C) 10 repeats of 208 bp, and (D) 10 repeats of 208 bp with histone H1 bound were cross-linked via H4-V21C/H2A-E64C disulfide formation under conditions causing compaction. The products of the reactions were separated by native APAGE before (lane 1) and after (lane 2) digestion with Sca I restriction endonuclease (markers, lane M). Cross-links were reduced with 100 mM DTT after cleavage to produce mononucleosomes (lane 3). The positions of starting material, cleaved species of maximum size, and mononucleosome are indicated. The higher bands (lane 1), present before cross-linking, represent less than 5% of the material. Arrays with 12 repeats of 172 bp gave compatible results (22). (E) Analytical comparison of Sca I cleavage products for a dodecanucleosome with theoretical values. The band intensities for 15 experiments (A) were quantified from the fluorescence intensity of the ethidium bromide stain (black). Error bars correspond to one standard deviation from the mean for multiple measurements. The band intensities for one-start (white) and two-start (gray) structures were calculated based on the measured yield of cysteine to disulfide conversion of 42.8%. (F) Analytical comparison of Sca I cleavage products for an H1-bound decanucleosome with theoretical values. The band intensities for five experiments (D) were quantified as for (E) (black). The theoretical values were calculated on the basis of the measured yield of 29.9%.

Nonreducing SDS-PAGE followed by Coomassie Blue gel staining was used to estimate the fraction of cysteine sulfhydryl groups in disulfide bridges. Quantification of the band patterns for uncrosslinked and cross-linked samples resulted in a value of $42.8\% \pm 4.7\%$ (for example, Fig. 2, lane 2). With this disulfide yield, bands corresponding to DNA lengths greater than one-half the initial number of repeats would be expected for a one-start nucleosome arrangement. Comparison of the observed with the theoretical fragment distributions for two-start and one-start structures shows that the dodecanucleosome (Fig. 3A) has a two-start geometry (Fig. 3E). Disulfide cross-linking of decanucleosomes with histone H1 incorporated resulted in a cross-linking yield of $29.9\% \pm 5.0\%$, sufficient to reveal a fragmentation pattern also indicative of two-start geometry (Fig. 3, D and F).

Assuming random formation of up to two disulfide bonds per nucleosome-nucleosome interface, the measured yields of disulfide formation suggest cross-linking probabilities ($2p-p^2$) of 76.3% ($p = 42.8\%/83.3\%$) and 55.6% ($p = 29.9\%/83.3\%$) for arrays compacted with divalent cation and H1, respectively. The corresponding fits ($R = 0.949$ and $P = 0.004$ and $R = 0.980$ and $P = 0.003$) of the observed gel distributions with those calculated for two-start organization validates this model. The lack of complete cross-linking suggests that disulfide formation depends on static disorder or dynamic fluctuations of nucleosomes within the higher order structure.

We have directly imaged the cross-linked arrays by electron microscopy (EM) to complement the native APAGE analysis. To see the direction of the fiber axis clearly, we prepared mutant arrays with a mean length

of 48 repeats (48-mer) of 177 base pairs (bp) from ligated dodecamer DNA. After compaction with concurrent disulfide crosslinking, these arrays were applied to grids and negative-stained with uranyl acetate. Fixatives such as formaldehyde or glutaraldehyde were not used. The particles appear most frequently as two equal-length parallel rows with widths of ~ 25 to 30 nm (Fig. 4A). The rows correspond to a width of ~ 12 nm and are interpreted as nucleosomes stacked on their histone octamer faces, consistent with the cross-link experiments. The two rows are indicative of two-start organization. In contrast, when the cross-link is reversed by 100 mM DTT treatment, the particles lose their fiberlike appearance (Fig. 4B).

The APAGE experiments suggest that the nucleosomes in each of the fiber starts should be visible as separate stacks in electron micrographs after treatment with Sca I. Images of the 48-mer samples after Sca I digestion show that the fibers are indeed separable into single columns (Fig. 4C). The length of the columns is reduced compared with the undigested material because of incomplete internucleosome cross-linking. Furthermore, pairs of columns sometimes appear to be coupled at points, because the DNA connections introduced by DNA ligation are not Sca I-cleavable.

H1-bound 48-mer arrays fixed with formaldehyde and negative-stained reveal fibers with regions that are two-start in appearance (fig. S2A). These images have an appearance similar to those from studies using native chromatin (7, 14). Decanucleosomes disulfide-cross-linked with one copy of histone H1 bound per nucleosome clearly display two parallel stacks of nucleosomes (fig. S2, B and C). Evidently, the one-start versus two-start secondary structure organi-

zation of chromatin is not affected by the binding of one copy of the linker histone per nucleosome. In this regard, mass-corrected s values from sedimentation analysis measured for the dodecanucleosomes result in the same degree of compaction whether or not H1 is bound, despite the increased stability it affords (15). In vivo studies have shown that H1 is inessential for viability of one-cell eukaryotes (16–19) and that substoichiometric amounts of H1 are tolerated in mice (20), consistent with our results for the chromatin fiber based on nucleosome arrays. Additional specifics of the form(s) of the two-start structure (for example, Fig. 1, B and C) remain to be elucidated by cryo-EM and x-ray crystallography.

References and Notes

1. K. E. van Holde, *Chromatin, Springer Series in Molecular Biology*, A. Rich, Ed. (Springer-Verlag, New York, 1988).
2. K. Luger, A. W. Maeder, R. K. Richmond, D. F. Sargent, T. J. Richmond, *Nature* **389**, 251 (1997).
3. C. A. Davey, D. F. Sargent, K. Luger, A. W. Mäder, T. J. Richmond, *J. Mol. Biol.* **319**, 1097 (2002).
4. T. J. Richmond, J. Widom, in *Chromatin Structure and Gene Expression*, S. C. R. Elgin, J. L. Workman, Eds. (Oxford Univ. Press, Oxford, 2000), pp. 1–23.
5. Y. G. Strukov, Y. Wang, A. S. Belmont, *J. Cell Biol.* **162**, 23 (2003).
6. J. Widom, A. Klug, *Cell* **43**, 207 (1985).
7. C. L. F. Woodcock, L.-L. Y. Frado, J. B. Rattner, *J. Cell Biol.* **99**, 42 (1984).
8. J. T. Finch, A. Klug, *Proc. Natl. Acad. Sci. U.S.A.* **73**, 1897 (1976).
9. F. Thoma, T. Koller, A. Klug, *J. Cell Biol.* **83**, 403 (1979).
10. J. D. McGhee, J. M. Nickol, G. Felsenfeld, D. C. Rau, *Cell* **33**, 831 (1983).
11. A. Worcel, S. Strogatz, D. Riley, *Proc. Natl. Acad. Sci. U.S.A.* **78**, 1461 (1981).
12. S. P. Williams et al., *Biophys. J.* **49**, 233 (1986).
13. B. Dorigo, T. Schalch, K. Bystricky, T. J. Richmond, *J. Mol. Biol.* **327**, 85 (2003).
14. J. B. Rattner, B. A. Hamkalo, *Chromosoma* **69**, 363 (1978).
15. L. M. Carruthers, J. Bednar, C. L. Woodcock, J. C. Hansen, *Biochemistry* **37**, 14776 (1998).
16. X. Shen, L. Yu, J. W. Weir, M. A. Gorovsky, *Cell* **82**, 47 (1995).
17. H. G. Patterson, C. C. Landel, D. Landsman, C. L. Peterson, R. T. Simpson, *J. Biol. Chem.* **273**, 7268 (1998).
18. J. L. Barra, L. Rhounim, J. L. Rossignol, G. Faugeron, *Mol. Cell. Biol.* **20**, 61 (2000).
19. A. Ramon, M. I. Muro-Pastor, C. Scazzocchio, R. Gonzalez, *Mol. Microbiol.* **35**, 223 (2000).
20. Y. Fan et al., *Mol. Cell. Biol.* **23**, 4559 (2003).
21. J. Bednar, R. A. Horowitz, J. Dubochet, C. L. Woodcock, *J. Cell Biol.* **131**, 1365 (1995).
22. B. Dorigo, T. J. Richmond, data not shown.
23. We thank M. Müller and H. Gross for assistance with EM and V. Ramakrishnan for providing the H1 expression plasmid. We are grateful for financial support from the Swiss National Science Foundation through the National Center for Competence in Research Structural Biology and a grant to T.J.R.

Supporting Online Material

www.sciencemag.org/cgi/content/full/306/5701/1571/DC1

Materials and Methods

Figs. S1 and S2

Table S1

References

22 July 2004; accepted 6 October 2004

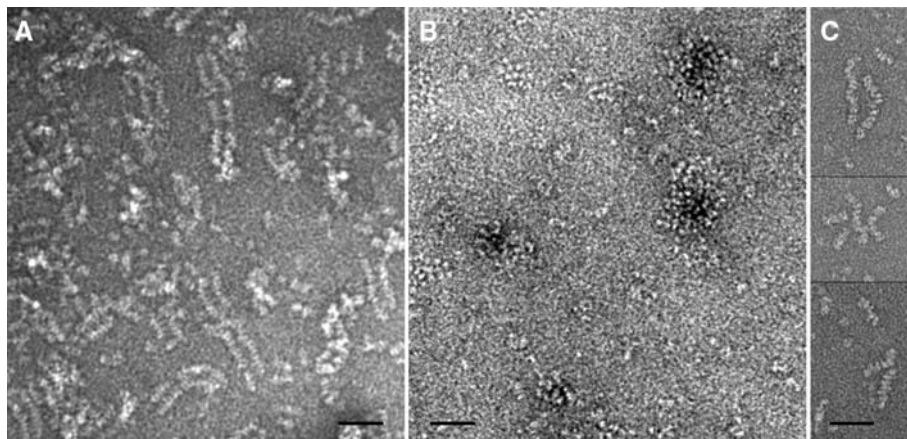


Fig. 4. Electron micrographs showing the two-start organization of nucleosome arrays. (A) 48-mer nucleosome arrays were cross-linked via H4-V21C/H2A-E64C-mediated disulfide formation under compacting conditions and prepared for EM with the use of negative stain. (B) Arrays were treated with 100 mM DTT to relieve the disulfide cross-link and then prepared as for (A). (C) Arrays (three separate examples are shown) prepared as for (A) were cleaved at the Sca I site in the linker DNA. Scale bars indicate 50 nm. EM magnification was 13,000 \times for (A) and (B) and 26,000 \times for (C).